Supporting Information

Controlling Stiction in Nano-Electro-Mechanical Systems Using Liquid Crystals

Oleksandr Buchnev [1], Nina Podoliak [1], Thomas Frank [1,2], Malgosia Kaczmarek [2], Liudi Jiang [3] and Vassili A. Fedotov[1,*]

[1] Optoelectronics Research Centre, University of Southampton, SO17 1BJ, UK

[2] Physics and Astronomy, University of Southampton, SO17 1BJ, UK

[3] Faculty of Engineering and the Environment, University of Southampton, SO17 1BJ, UK

*e-mail: vaf@orc.soton.ac.uk

1. Spectral shift due to LC phase transition

Below we provide an upper estimate for the expected spectral shift of the metamaterial resonance upon swithcing liquid crystal 5CB from the isotropic to nematic phase at 0 V.

Given that at zero electric field LC molecules in the nematic phase tend to align their long axis parallel to the length of the nano-wires [1, 2], the resonant optical field of the plasmons will 'see' the ordinary refractive index (n_o = 1.520 @ 1 μm). In this case the difference between the refractive indices of the isotropic (n_{iso} = 1.574) and nematic phases of 5CB is only 0.054, and therefore at 0 V the spectral detuning of the resonance may not exceed 3% (~ 40 nm). In reality, the shift is even smaller since the nano-wires rest on a high-index dielectric substrate (silicone nitride).

2. Changes of LC optical anisotropy induced by electric field

Here we model the changes in the optical anisotropy of nematic 5CB that were induced electrically as we ramped up the bias voltage.

Changes in the optical anisotropy of LC layer were modelled numerically, by simulating electrically induced re-orientation of LC molecules in the bulk of the layer. A schematic of the simulated domain is shown in Figure S1. It features four periods of the metamaterial gold wire grid on silicon nitride bridges (to account for alternating grouping of wire pairs) and a 2 μm thick layer of LC, with periodic boundary conditions applied to the domain's sidewalls.

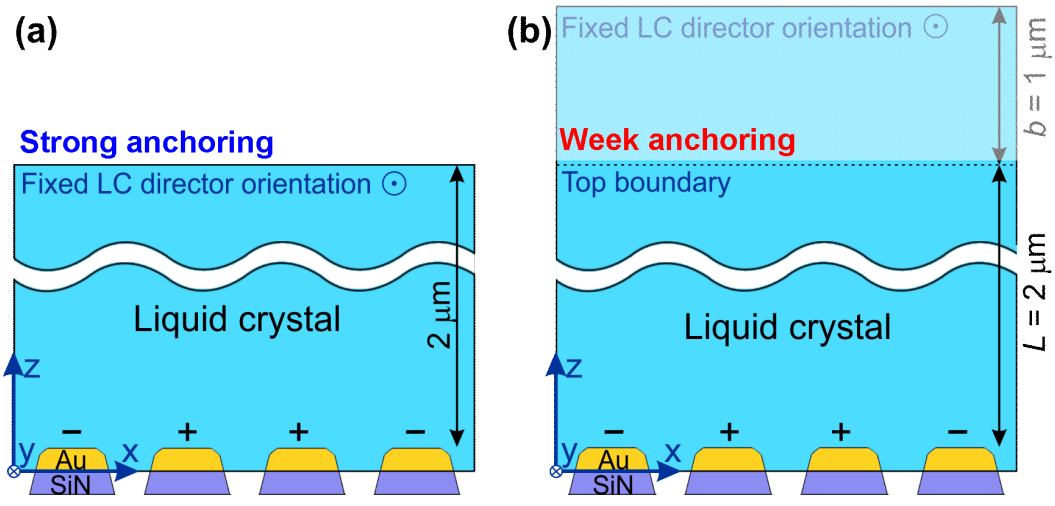

Figure S1. Schematics of the simulation domains that were used in conjunction with strong (a) and weak (b) anchoring – the two limiting cases of the boundary condition at the surface of the glass topping the LC layer. Symbols '+' and '–' indicate the sign of electrostatic potentials applied to gold wires.

The orientation of LC molecules was described via the nematic director $\mathbf{n}$, which is characterized by the tilt and twist angles, θ and φ. The tilt angle gives the deflection of the director out of the xy-plane, while the twist angle describes the director orientation in the xy-plane. Using Frank-Osen continuous theory, the spatial distribution of LC director can be characterized by the free-energy functional:

$$F = \int_V \left\{ \frac{K_1}{2}\left(\nabla \cdot \mathbf{n}\right)^2 + \frac{K_2}{2}\left(\mathbf{n} \cdot \left[\nabla \times \mathbf{n}\right]\right)^2 + \frac{K_3}{2}\left(\mathbf{n} \times \left[\nabla \times \mathbf{n}\right]\right)^2 - \frac{1}{2}\varepsilon_0 \Delta\varepsilon \left(\mathbf{E} \cdot \mathbf{n}\right)^2 \right\} dV \,, \quad (1)$$

where K_1, K_2 and K_3 are the elastic constants of the liquid crystal and $\Delta\varepsilon$ is the DC dielectric anisotropy ($\Delta\varepsilon = \varepsilon_{\parallel} - \varepsilon_{\perp}$ and $\varepsilon_{\parallel}$, $\varepsilon_{\perp}$ are the dielectric constant in the direction parallel and perpendicular to the LC director). The spatial dependences of the tilt and twist angles, $\theta(x, z)$ and $\varphi(x, z)$ were calculated by minimizing the free-energy functional (1) across the domain using the finite-element method implemented in Comsol Multiphysics®.

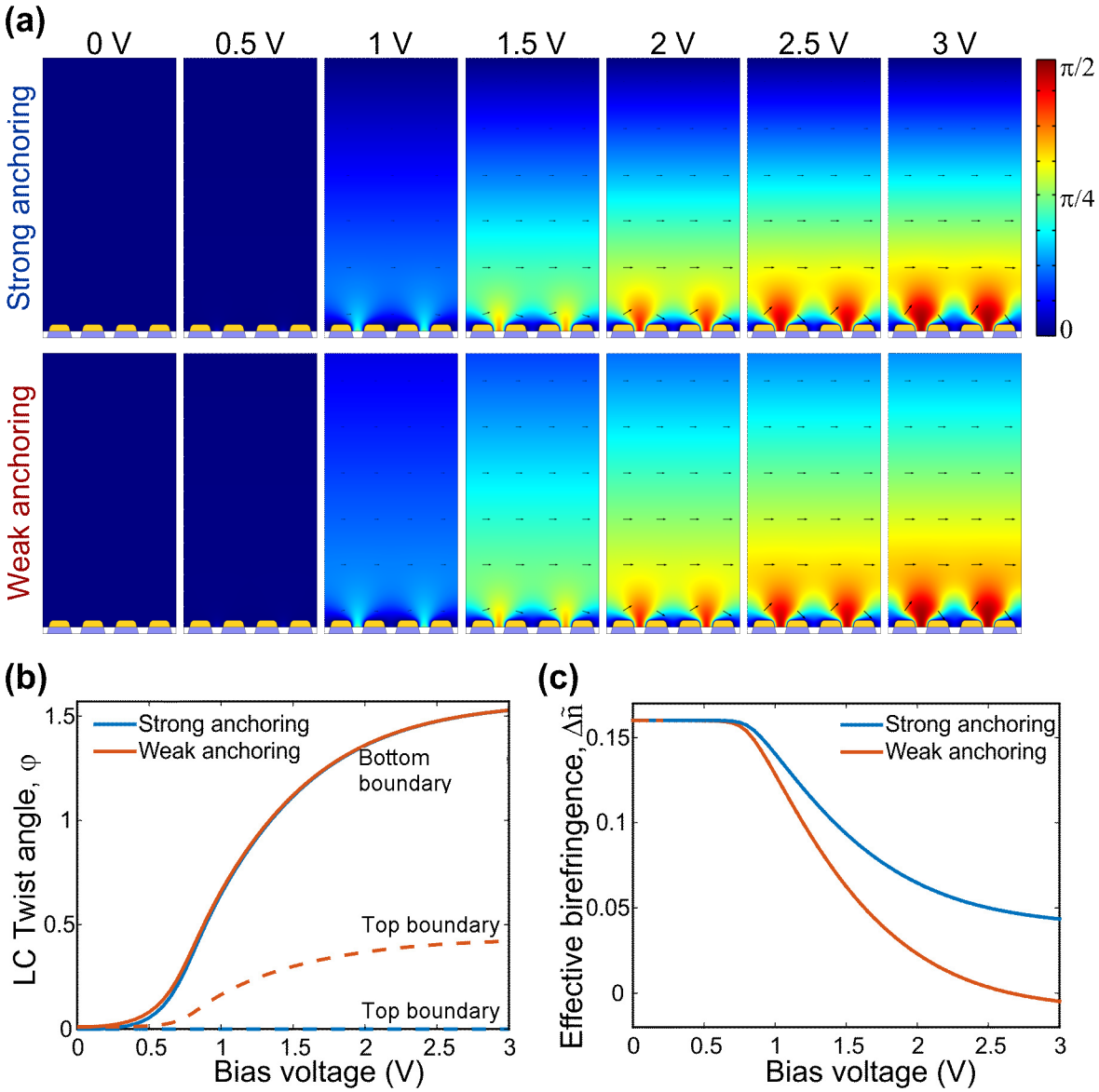

Figure S2. (a) Spatial distribution of LC twist angle simulated at different levels of applied voltage for the case of strong and weak LC anchoring at the top boundary. (b) Twist angle at the top and bottom boundaries of the simulation domain as a function of applied voltage. (c) Effective birefringence of the LC layer calculated as a function of applied voltage for the case of strong and weak anchoring.

Based on previous experimental findings [1, 2], we assumed strong anchoring of LC molecules at the surfaces of gold wires with the local orientation of LC director being parallel to the length of the wires. In the modelled geometry this was enforced by setting $\theta = 0$ and $\varphi = 0$ at the gold-LC interface. We also assumed that LC partially infiltrated the gaps between silicon nitride bridges and formed a free flat surface terminating at the border between the bridges and wires [3]. Weak LC anchoring at the domain's top boundary was emulated by introducing an additional layer of LC with the extrapolation thickness b [4] (as shown in Figure S1b), where $b = K_2/W_s$, and W_s is the surface anchoring energy. The initial alignment of LC molecules at the top boundary was parallel to the y-axis, i.e. $\theta = 0$ and $\varphi = 0$. For comparison, we also considered the case of strong LC anchoring by applying fixed boundary conditions $\theta = 0$ and $\varphi = 0$ at the top boundary. The following constants (provided by Merck) were used in our model to describe the behaviour of liquid crystal 5CB in the nematic phase: K_1 = 6.5 pN, K_2 = 4.1 pN, K_3 = 9.5 pN, $\varepsilon_{||}$ = 17.9, $\varepsilon_{\perp}$ = 6.9. The results of our simulations are presented in Figure S2.

Figure S2a shows the spatial variation of the twist angle, φ, for the case of strong ($W_s \to \infty$) and weak (W_s = 4.1 x 10^{-6} N/m, b = 1 μm) anchoring, and applied voltage in the range 0 – 3 V. In both cases the alignment of LC is planar at 0 V and 0.5 V with the director being oriented parallel to the y-axis (i.e. $\varphi = 0$). At 1 V, which is just above the Fréedericksz transition, the distortion of LC is seen to propagate towards the top boundary, and the twist of LC layer becomes evident at 1.5 V. At 3 V the director is fully re-oriented in both cases, signifying the saturation of the twist angle at the value of $\pi/2$. The saturation at 3 V is more apparent in Figure S2b, which presents the evolution of the twist angle as a function of the bias voltage at the bottom boundary, between oppositely charged gold wires, and the top boundary. Note that in the case of strong anchoring the twist angle does not change at the top boundary due fixed boundary condition $\theta = 0$ and $\varphi = 0$.

Changes in the optical anisotropy of LC layer, caused by the re-orientation of LC molecules, is convenient to described in terms of effective birefringence of the layer, calculated as

$$\Delta\tilde{n} = \frac{1}{L}\int_0^L \left(n_y(z) - n_x(z)\right) dz \,, \tag{2}$$

where n_x and n_y are the refractive indices averaged over one period of the metamaterial wire grid. The field-induced re-orientation of LC molecules in the xy-plane leads to a decrease of n_y and increase of n_x, which corresponds to a decrease of the effective birefringence, as shown in Figure S2c. Evidently, for both strong and weak anchoring cases, most of the change occurs below 2 V, while the dependence saturates by 3 V.

3. Control electric field and electrostatic attraction between gold nano-wires

Below we model the spatial distribution of the control electric field and the corresponding electrostatic attraction, and present their evolution with increasing bias voltage.

Our model was also used to obtain the spatial distribution of the control electric field, $\mathbf{E}(x, z)$, which had been coupled with the functional (1) through LC-dielectric tensor. Figure S3a shows the profiles of electric field in the vicinity of two oppositely charged gold wires, which were calculated for the nematic and isotropic ($\varepsilon_{iso} = \varepsilon_{||}/3 + 2\varepsilon_{\perp}/3$) phases of 5CB. While in the isotropic phase the strength of electric field is simply proportional to the applied voltage, in the nematic phase the spatial distribution of electric field becomes also affected, following the changes in the anisotropy of LC dielectric tensor the field induces. We also calculated electrostatic attraction between the wires (assuming they did not move) in the isotropic and nematic phases by means of the Maxwell stress tensor. Figure S3b shows that above 1 V the wires are pulled towards each other stronger in the nematic rather than isotropic phase, and the lead only increases with increasing bias voltage.

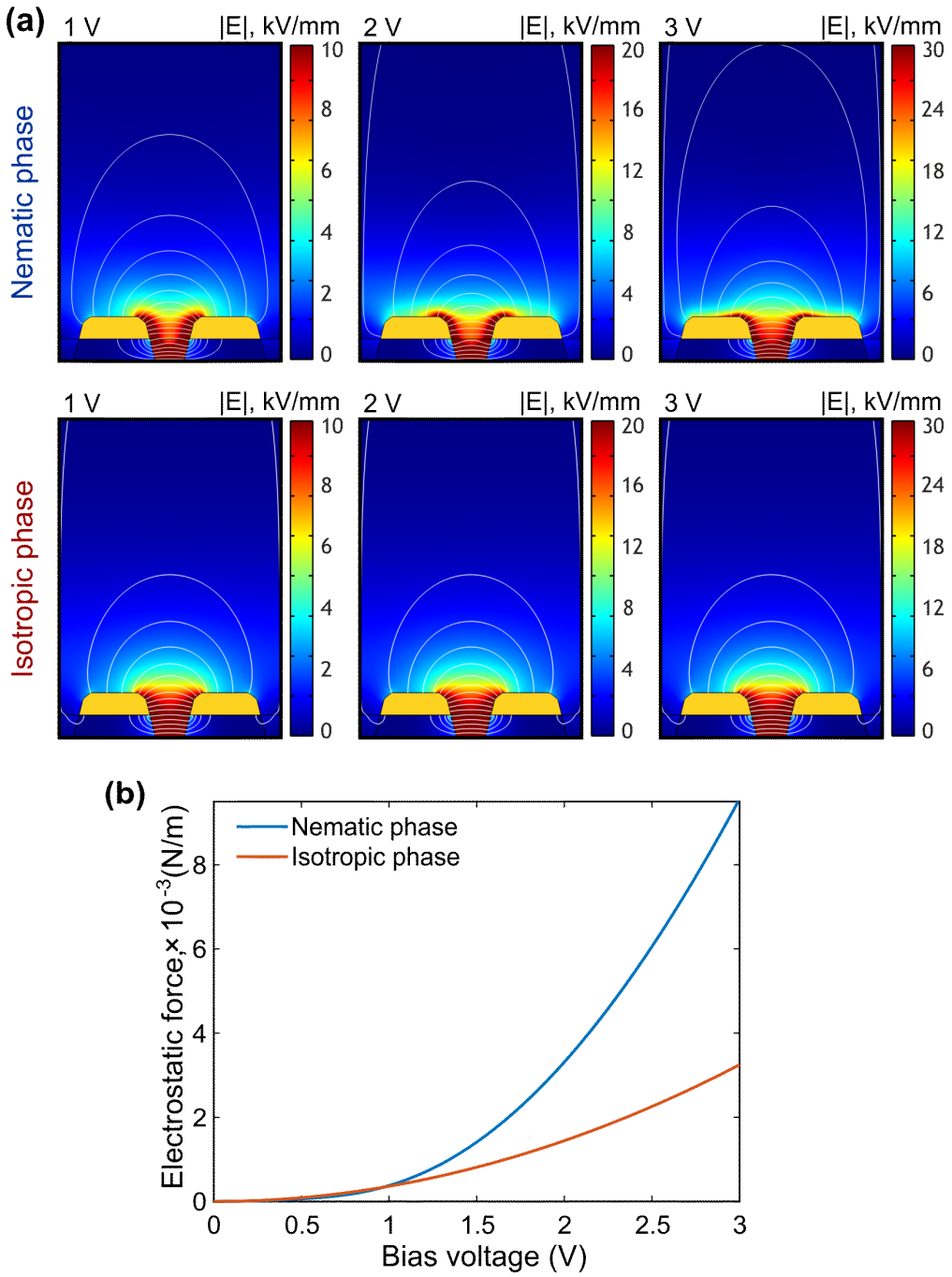

Figure S3. (a) Distribution of electric field (colour map) near two oppositely charged gold wires calculated for the case of the nematic and isotropic phase of 5CB. White lines visualise electric field lines. (b) Strength of the electrostatic attraction between the gold wires in nematic and isotropic LC as a function of the applied voltage.

References

[1] P. N. Sanda, D. B. Dove, H. L. Ong, S. A. Jansen, and R. Hoffmann, "Role of surface bonding on liquid-crystal alignment at metal surfaces", Phys. Rev. A **39**, 2653 (1989).

[2] O. Buchnev, J. Y. Ou, M. Kaczmarek, N. I. Zheludev, and V. A. Fedotov, "Electro-optical control in a plasmonic metamaterial hybridised with a liquid-crystal cell", Opt. Express **21**, 1633 (2013).

[3] O. Buchnev, N. Podoliak, M. Kaczmarek, N. I. Zheludev, and V. A. Fedotov, “Electrically controlled nanostructured metasurface loaded with liquid crystal: toward multifunctional photonic switch,” Adv. Optical Mater. **3**, 674 (2015).
[4] X. Nie, R. Lu, H. Xianyu, T. X. Wu, and S.-T. Wu, “Anchoring energy and cell gap effects on liquid crystal response time,” J. Appl. Phys. **101**, 103110 (2007).